

Fermi National Accelerator Laboratory

FERMILAB-Pub-94/029

A Low-Pressure, Micro-Strip Gas Chamber Operated with Secondary-Electron Emission

D.F. Anderson and S. Kwan

*Fermi National Accelerator Laboratory
P.O. Box 500, Batavia, Illinois 60510*

M. Salomon

*TRIUMF
4004 Wesbrook Mall, Vancouver, Canada V6T 2A3*

February 1994

Submitted to *Nuclear Instruments and Methods A*

Disclaimer

This report was prepared as an account of work sponsored by an agency of the United States Government. Neither the United States Government nor any agency thereof, nor any of their employees, makes any warranty, express or implied, or assumes any legal liability or responsibility for the accuracy, completeness, or usefulness of any information, apparatus, product, or process disclosed, or represents that its use would not infringe privately owned rights. Reference herein to any specific commercial product, process, or service by trade name, trademark, manufacturer, or otherwise, does not necessarily constitute or imply its endorsement, recommendation, or favoring by the United States Government or any agency thereof. The views and opinions of authors expressed herein do not necessarily state or reflect those of the United States Government or any agency thereof.

A Low-Pressure, Micro-Strip Gas Chamber Operated with Secondary-Electron Emission

D.F. Anderson ¹, S. Kwan ¹, and M. Salomon ²

¹ Particle Detector Group

Fermi National Accelerator Laboratory

Batavia, IL 60510 U.S.A.

and

² TRIUMF

4004 Wesbrook Mall

Vancouver, B.C., Canada V6T 2A3

(To be submitted to Nuclear Instruments and Methods A)

Abstract

The operation of a low-pressure micro-strip gas chamber with a thick CsI secondary-electron emitting surface as the source of primary ionization is presented. Fast signals are produced and improvements in gain and timing resolutions of over an order of magnitude, compared to atmospheric devices, are achieved with reduced sensitivity to discharges. Such devices should have little or no angular dependence in their position and timing resolution, or on their efficiency.

1 Introduction

Currently there is a great deal of activity in the development of the micro-strip gas chamber, MSGC. (See ref. [1] for an excellent compilation of much of the work in the field.) The key features of the MSGC are that they have good position resolution (30-40 μm rms), high rate capability ($>10^6 \text{ mm}^{-2}\text{s}^{-1}$), and can sustain doses of 10 Mrad. Such a dose corresponds to operation in an LHC environment for as long as 20 years. The MSGC is also lends itself to the coverage of large areas.

At present the MSGC has its shortcomings. One problem is the relatively low gains that are achievable. Gains on the order of 3000 are considered safe while a gain of 10^4 is considered exceptional due to the risk of discharge[1]. A low gain requires the use of low noise amplifiers and also impacts the efficiency of the MSGC for particles with inclined tracks.

Another problem of the MSGC for operation at the LHC, with its 25 ns bunch-crossing time, is that it takes 50-70 ns to collect the initial ionization produced across the gap. Thus the shaping time of the amplifiers must be made sufficiently long to collect the charge, or the gap must be made smaller. The latter solution can be done at the expense of efficiency. At present the amplifier shaping time must be 40-50 ns to maintain high efficiency. The primary charge being distributed randomly across the gap also places a limitation on the timing resolution because of the fluctuations in the arrival time of the first charge cluster. A resolution of 10.6 ns rms has been achieved using a short shaping time, fast gas, a large drift field, and a constant-fraction discriminator[2]; while resolutions of ≥ 17 ns are measured with more practical configurations[1].

The MSGC is also sensitive to the angle of the incident particle. In a measurement that obtained a timing resolution of 17 ns at 0° [1], the resolution degraded to 27 ns at 10° . A measurement of the position resolution of 40 μm at 0° resulted in a resolution of only 300 μm at 30° [3]. Efficiency also degrades as the angle increases. For a threshold of about one primary electron, the efficiency of a single strip has been measured to drop from about 98% at 0° to below 35% at 30° [3].

We have addressed these problems by going to a low-pressure mode of operation with most of the primary charge produced by secondary-electron emission, SEE, from the front surface of the chamber. The low-pressure operation, which allows one to amplify the charge across the entire gap, greatly increases the maximum gain and reduces the sensitivity of the gas in the gap to passing particles. The production of the charge from a surface by SEE improves the collection time and removes the problems associated with particles passing through the MSGC at an angle.

2 Secondary-electron emission studies

One of the keys to the low-pressure operation of the MSGC is the production of the primary charge by SEE. When a charged particle passed through a thin foil, secondary electrons are sometimes emitted. Earlier work on SEE chambers were done in vacuum with electron amplification achieved in a micro channel plate[4]. Recent interest in SEE has focused on coupling secondary-electron emitters to a low-pressure gas detector[5-8], in which case the secondary electrons are amplified in the gas.

For most materials, the SEE efficiency is on the order of a few percent. On the other hand, alkali halides such as CsI and KCl have long been known to be good secondary-electron emitters[9, 10]. A thin layer of porous CsI in a vacuum, for example, can give 3-5 electrons per passing charged particle[9, 11, 12]. We have studied secondary electron emission as function of gas pressure and thickness for several emitters. The experimental setup for the SEE measurements is shown schematically in fig. 1. It consists of a simple parallel-plate chamber with one electrode made of aluminum and the other made from a flat resistive-glass plate, separated by a 1.6 mm gap. The aluminum electrode has a thin window which is coated with a thick layer of alkali-halide deposited under vacuum or sprayed on in air[6]. Beta particles from a ^{90}Sr source entered the chamber through a thin window and passed through the aluminum electrode and the secondary-electron emitter. With the chamber biased such that the Al is the cathode, secondary electrons from the alkali halide emitter are detected. With the bias reversed only the gas contribution is detected. The SEE contribution of the aluminum window is known to be small. The difference was used in determining the efficiency of the emitter being studied. Ethane and isobutane were used in the studies. The performances of both gases were comparable, and so only the ethane results are presented here. The best results were achieved when the emitting material was heated in the evacuated chamber for several hours previous to the measurement.

Fig. 2 shows the SEE pulse-height spectrum of this chamber with 10 μm CsI as the emitter, and with the bias reversed. The gas filling was 20 torr ethane and the bias voltage was 600 V. Data were collected with both biases for the same length of time. The SEE spectrum has had the reverse-biased spectrum subtracted to remove the effect of the gas. The estimate of the average number of secondary electrons per beta particle is 3.5 ± 0.5 . The average number of electrons is estimated by comparing the mean of the pulse-height spectrum with the mean from a single electron spectrum. Unfortunately, the efficiency of SEE is not what one would infer from Poisson statistics, with the probability of producing zero secondary electrons being larger than would be assumed by the mean

number of electrons detected [12]. Chianelli et al. measured an efficiency of 62% when the average number of secondary electrons was 4. This is consistent with our results.

Studies of the effect of the thickness of the CsI coating under different gas pressures were also made. Fig. 3. shows the relative efficiency for three thicknesses of CsI and for bare aluminum as a function of ethane pressure. At each pressure the voltage was increased until the efficiency reached a plateau. All the data points are normalized to the rate observed when the gas filling was 1 atmosphere of Ar-10% ethane. One can see that at low pressure, the effect of the CsI emitter is dominant while the direct ionization of the gas becomes dominant as the gas pressure goes up.

3 MSGC experimental procedures

The MSGC experimental setup is shown schematically in fig. 4. The anodes and cathodes are made of 1.1 μm thick aluminum traces on borosilicate glass. The anode and cathode traces (manufactured at Simon Fraser University, by Glenn Chapman) are 20 μm and 90 μm wide, respectively, with a 390 μm pitch. The surface of the glass plate, with electrodes, is covered with a 50 nm layer of Ni/NiO (50%/50%) to produce a highly resistive, ohmic surface[2]. For our measurements all 34 anodes were connected together to make a single electrode resulting in a rather high capacitance of about 90 pF.

The secondary-electron emitter was placed on a thin aluminum support above the glass plate. The MSGC was operated with two gap sizes: 2 mm and 1.2 mm. For the tests made at atmospheric pressure the gas mixture was argon/ethane (90% / 10%). In all cases, 10 μm CsI secondary-electron emitters were used.

4 Experimental results

The low-pressure MSGC operated very well with only an occasional discharge due to dust particles on the traces. Although gains were often pushed to the discharge point, the nature of the low-pressure operation and the coating [2] seemed to have protected the chamber from damage.

When the three electrodes are connected to preamps with long shaping times, the time for the signal to develop, and in particular the collection time of the positive ions can be seen. Fig. 5 shows oscilloscope traces from the emitter (e), cathode (c), and anode (a) from inverting, charge-sensitive amplifiers with the same gain and 5 μs shaping times. The gap was 2 mm, the gas filling was 20 Torr of ethane. The voltages on the emitter, V_e , and on the anode, V_a , were -540V and +90V, respectively. The cathodes were at ground potential. From the anode signal one sees a fast component with a rise time of less than 30 ns and a longer component with a collection time of about 700 ns. The fast

component contains over half of the total charge. Fig. 6 shows three similar traces but for a chamber with a gap of 1.2 mm. V_e and V_a were -485V and +90V, respectively. Here the collection time of the positive ions is reduced to less than 300 ns. This is about an order of magnitude shorter than for a conventional MSGC. Fig. 7 shows a typical pulse using an amplifier with a short shaping time. The rise time is about 3 ns, probably limited by the large capacitance of the MSGC. The double peak seen on the pulse is an electronic artifact.

One of the advantages of the low pressure operation is that most of the charge gain takes place in parallel-plate amplification across the gap and not in the small volume near the anode, as in atmospheric devices. This allows for much higher gains. Fig. 8 shows the collected charge and (minimum estimated) gain curves as a function of the voltage between the emitter and the anode, V_e+V_a , for various ethane pressures, and operated with the 2 mm gap. For all the measurements $V_a=250$ V and the cathodes were at ground potential. The gain was estimated by dividing the collected charge by 3, though the secondary-electron emitter for this measurement was inferior to our best emitters and probably was producing less than 3 electrons on average. Gains of several 10^4 and approaching 10^5 were measured. For comparison, the same MSGC operated at 1 Atm of argon-10% ethane gave a maximum gain of about 3×10^3 . Fig. 9 shows the collected charge as a function of V_e+V_a for gaps of 2 mm and 1.2 mm. (For the measurements $V_a=200$ V.) Except for the lower voltages needed for the smaller gap, the maximum charge for the two gaps is comparable.

Given that the initial charge is localized to the front surface, that there is essentially no variation in distances traveled to the anodes, and that ion mobility is high at low pressures, one would expect a significant improvement in the timing resolution of a low-pressure MSGC. Measurements were made using a 2 mm thick plastic scintillator to give a start signal. The amplifier used to make fig. 7 was also used. Fig. 10 shows the timing spectrum for a filling of 20 Torr of ethane, a 2 mm gap, and V_e and V_a equal -500V and 200V, respectively. The second peak is obtained by introducing an additional 8 ns of delay to the stop signal for a second measurement to provide a calibration and to set the scale for the eye. The average resolution for the two measurements is 0.94 ns rms. These measurements are dominated by geometric effects, and are very similar to the timing resolution measured with SEE and a low-pressure, resistive-plate chamber[5].

5 Discussion

We have shown that a low-pressure MSGC operated with SEE as the source of primary ionization offers high gains and a fast signal with excellent timing resolution,

and reduced sensitivity to discharge. One obvious shortcoming of this study is that our measurements were made with a beta source instead of a test beam. This adds an uncertainty to the number of secondary-electrons produced on the average. With a test beam we would also be able to measure the efficiency to the SEE.

We will implement individual anode readout in the future, thereby studying the angular dependence of position and timing resolution. Since our source of electrons is SEE it seems likely that when we are able to make these measurements, we will find a great improvement over the performance of conventional MSGC. The timing and position resolution should not be dependent on the angle of the track. In fact, SEE has been shown to improve with increased angle [7], thus the efficiency for passing particles should actually increase with increasing angle. We hope to make the measurements of efficiency, position and timing resolution, and angular dependence in a test beam at TRIUMF.

One serious problem of the low-pressure is that the MSGC must now be placed between two thin vacuum windows. This is a design problem as well as introducing additional mass. If several planes of readout are used it is hoped that thin kapton windows will not add much to the "material budget". Since the gains are considerably higher than for conventional MSGC, two-sided readout may be more practical and thus help to reduce their mass.

A second problem of the low-pressure MSGC is that one must rely on SEE as the source of initial ionization. The problem with SEE is that it does not obey Poisson statistics and yields an efficiency lower than would be expected from the mean number of electrons produced per particle. At the moment, we estimate our efficiency with a CsI emitter to be 50-60%. We believe that we will soon be able to report on a substantial improvement in the field of SEE which will yield a low-pressure MSGC with near unity efficiency. It has also been suggested [13] that if we do succeed with a high-yield SEE, that an atmospheric filling of helium and a quench gas be tried. This would solve the problems of working at low pressures.

Since at low pressure we are working in a different mode of amplification, the design of the MSGC must be rethought. Work on better designs and on good secondary-electron emitters may yield a good, compact, time-of-flight detector designed around the elements of a MSGC.

Acknowledgments

The authors would like to acknowledge the efforts of G. Chapman at the School of Engineering Science, Simon Fraser University in the manufacture of the prints used in this work. We would also like to thank C. Hojvat, F. Sauli, and S. Pordes for useful and stimulating discussions.

References

1. RD-28 Collaboration, CERN/DRDC/93-34, 1993.
2. M. Salomon, et al., IEEE Trans. on Nucl. Sci. to be published in NS-41 (1993) .
3. F. D. v. Berg, et al., IIHE/93-07, 1993.
4. J. C. Faivre, et al., IEEE Trans. on Nucl. Sci. NS-24 (1977) 299.
5. D. F. Anderson, S. Kwan, and V. Peskov, High Counting Rate Resistive-Plate Chamber, Third London Conference on Position-Sensitive Detectors London, September 6-10, 1993), vol. Fermilab-Conf-93/215,
6. D. F. Anderson, S. Kwan, and V. Peskov, Nucl. Instr. and Meth. A326 (1993) 611.
7. R. Chechik, et al., WIS-93/63/July-PH, 1993.
8. I. Frumkin, et al., Nucl. Instr. and Methods A329 (1993) 337.
9. W. Braunschweig, Phys. Scripta 23 (1981) 384.
10. M. P. Lorikian, et al., Nucl. Instr. and Methods 122 (1974) 377.
11. A. Breskin, Nucl. Instr. and Methods 196 (1982) 11.
12. C. Chianelli, et al., Nucl. Instr. and Methods A273 (1988) 245.
13. F. Sauli, private communication

Figure captions

- Fig. 1 Schematic of experimental setup used for SEE studies.
- Fig. 2 Pulse-height spectra for secondary-electron emission from 10 μm of CsI with the shown gas contribution (reversed bias) subtracted. The gas filling was 20 Torr of ethane.
- Fig. 3 Relative efficiency as a function of ethane pressure for 0.1, 1, and 10 μm of CsI and for bare aluminum, compared to 1 Atm of Ar-10% ethane and no secondary-electron emitter.
- Fig. 4 Schematic of the low-pressure MSGC.
- Fig. 5 Oscilloscope traces from the emitter (e), cathode (c), and anode (a) from inverting amplifiers with the same gain and 5 μs shaping times. The gap is 2 mm and the gas filling is 20 Torr of ethane.
- Fig. 6 Oscilloscope traces from the emitter (e), cathode (c), and anode (a) from inverting amplifiers with the same gain and 5 μs shaping times. The gap is 1.2 mm and the gas filling is 20 Torr of ethane.
- Fig. 7 Oscilloscope trace for a single pulse from the anode with an amplifier with a short shaping time.
- Fig. 8 Collected anode charge and estimated minimum gain as a function of the difference in V_e and V_a for various ethane pressures. V_a is held at +250V and V_e is negative polarity.
- Fig. 9 Collected anode charge as a function of the difference in V_e and V_a for 1.2 mm and 2.0 mm gaps. The ethane pressure is 20 Torr.
- Fig. 10 Timing spectrum for the MSGC with a 2 mm gap, and 20 Torr of ethane and with an 8 ns delay added for calibration. The fitted Gaussian curves are shown with indicated σ_{rms} resulting from the fits.

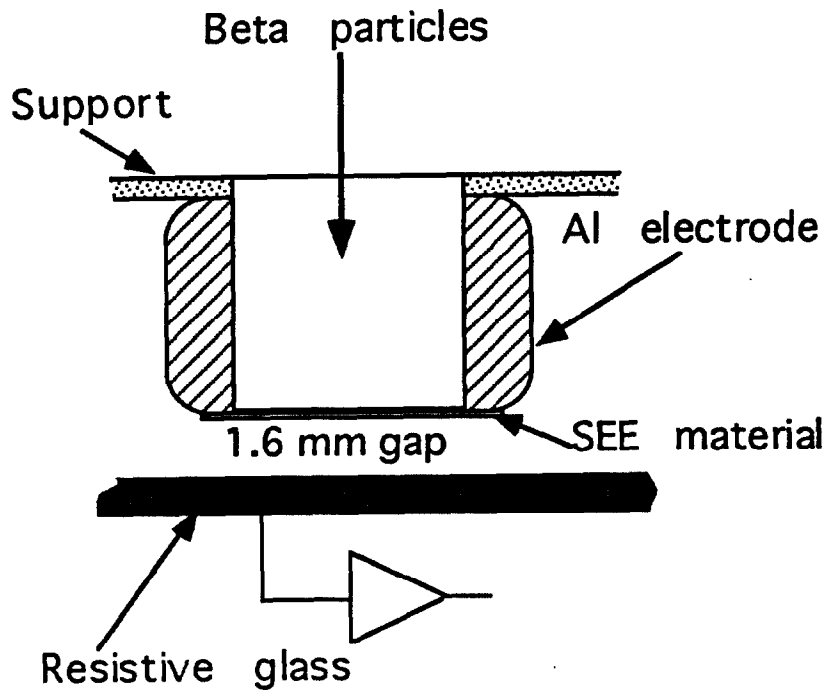


Figure 1

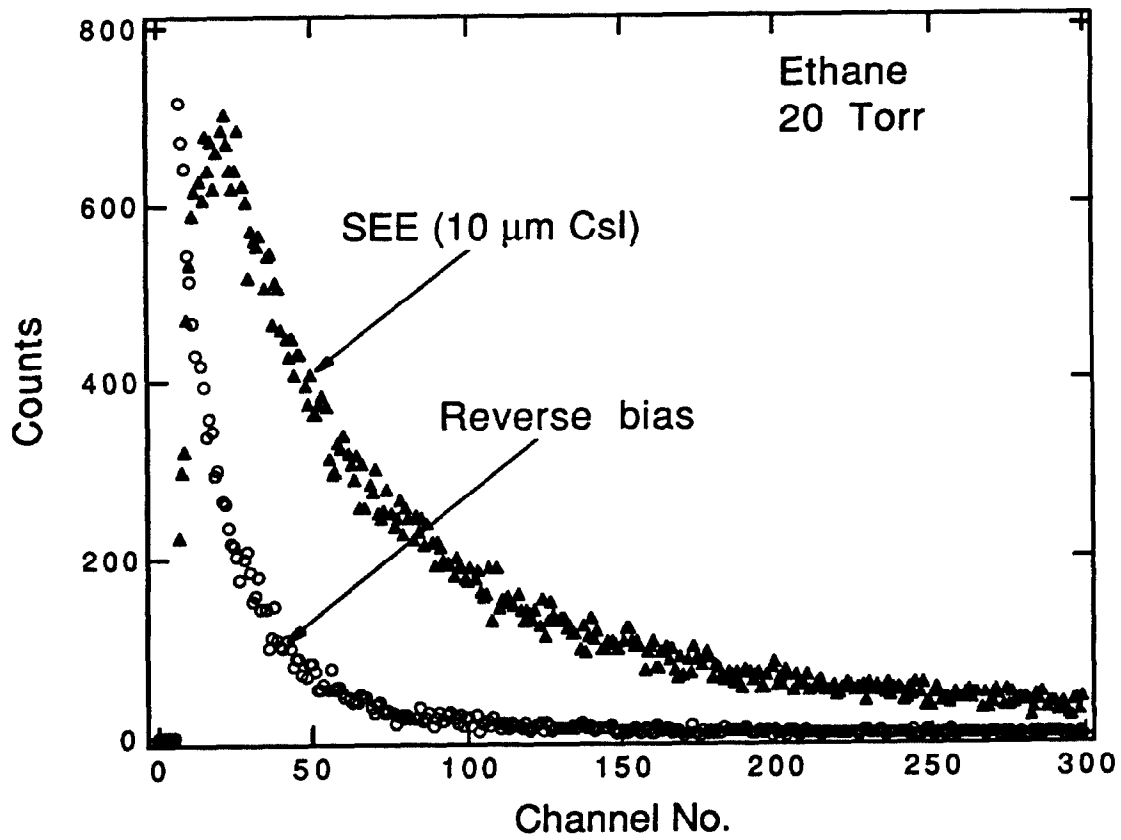


Figure 2

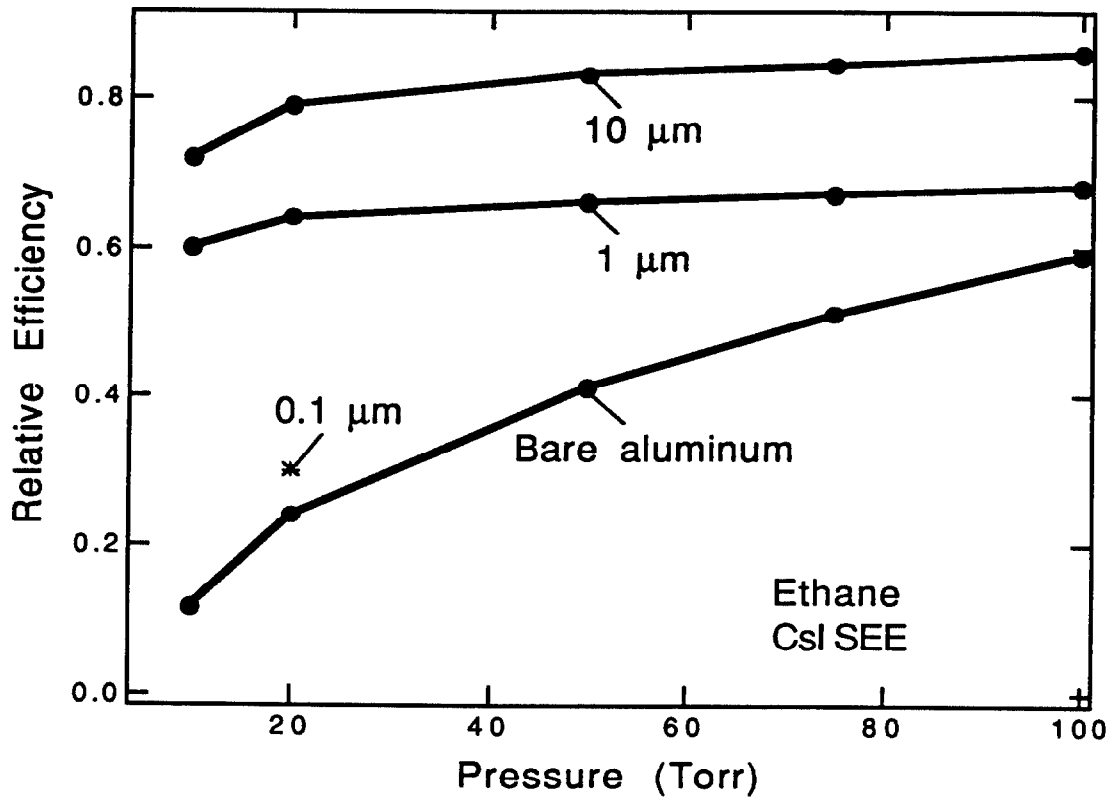


Figure 3

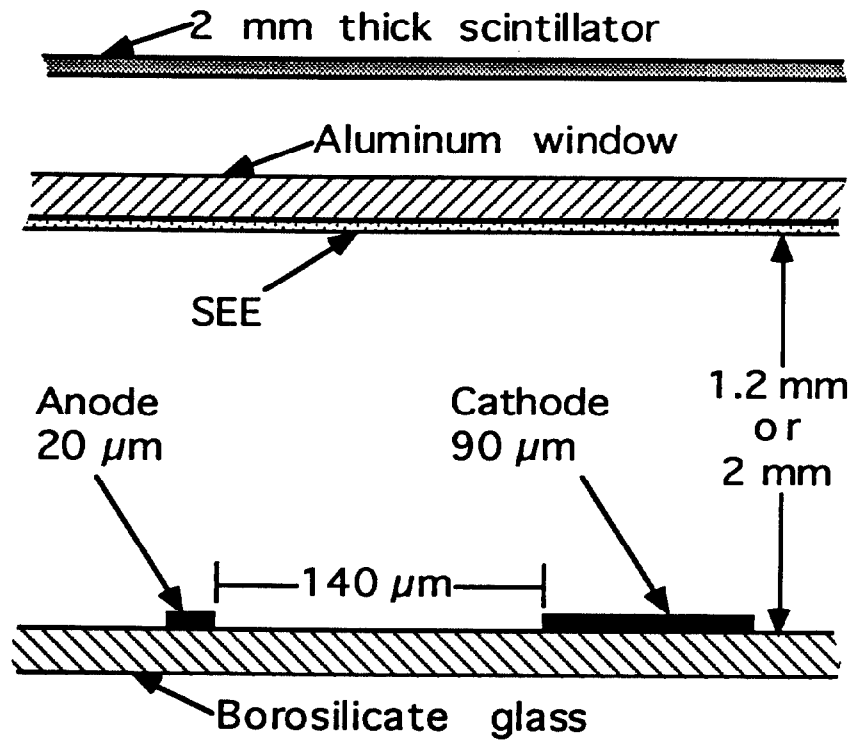


Figure 4

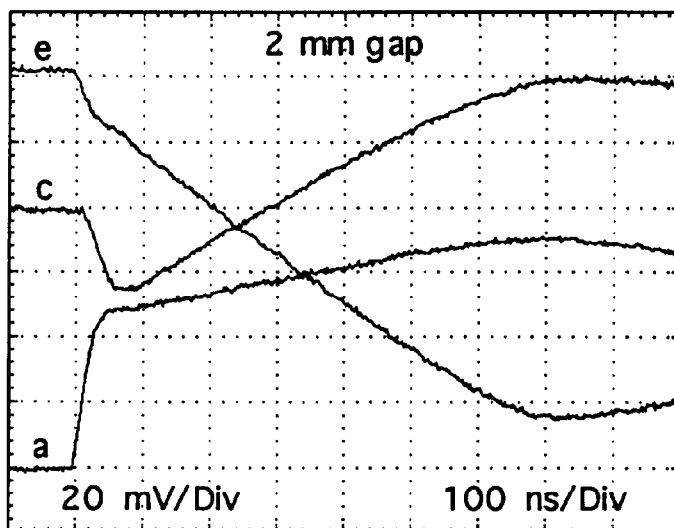


Figure 5

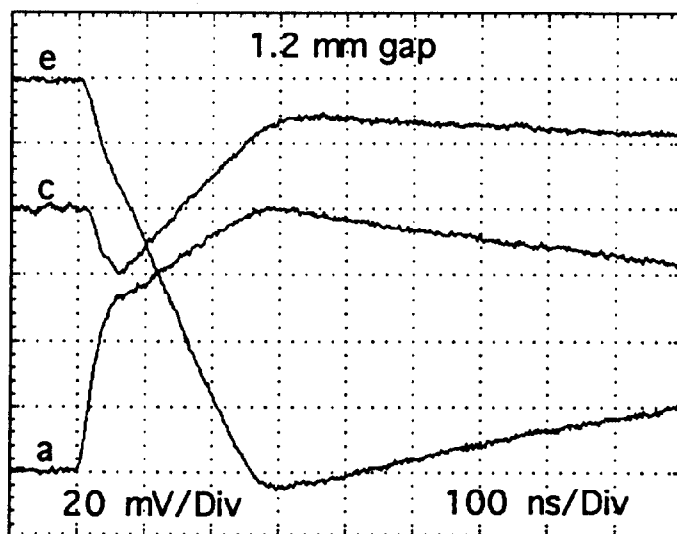


Figure 6

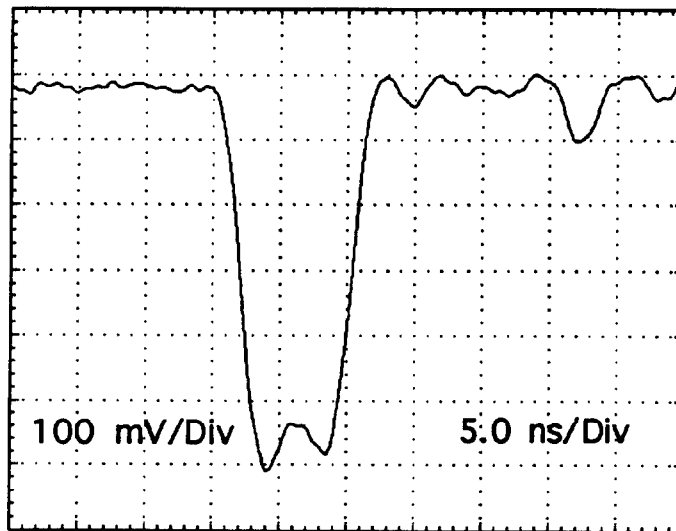


Figure 7

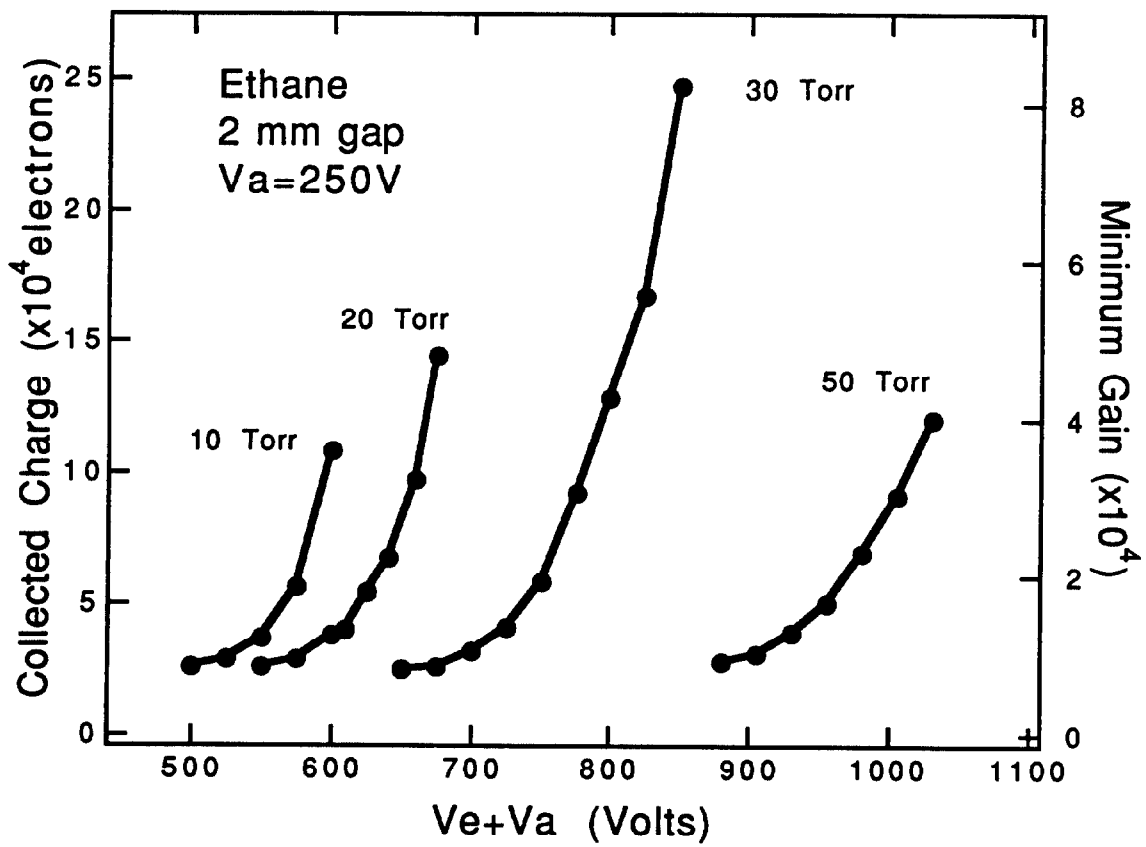


Figure 8

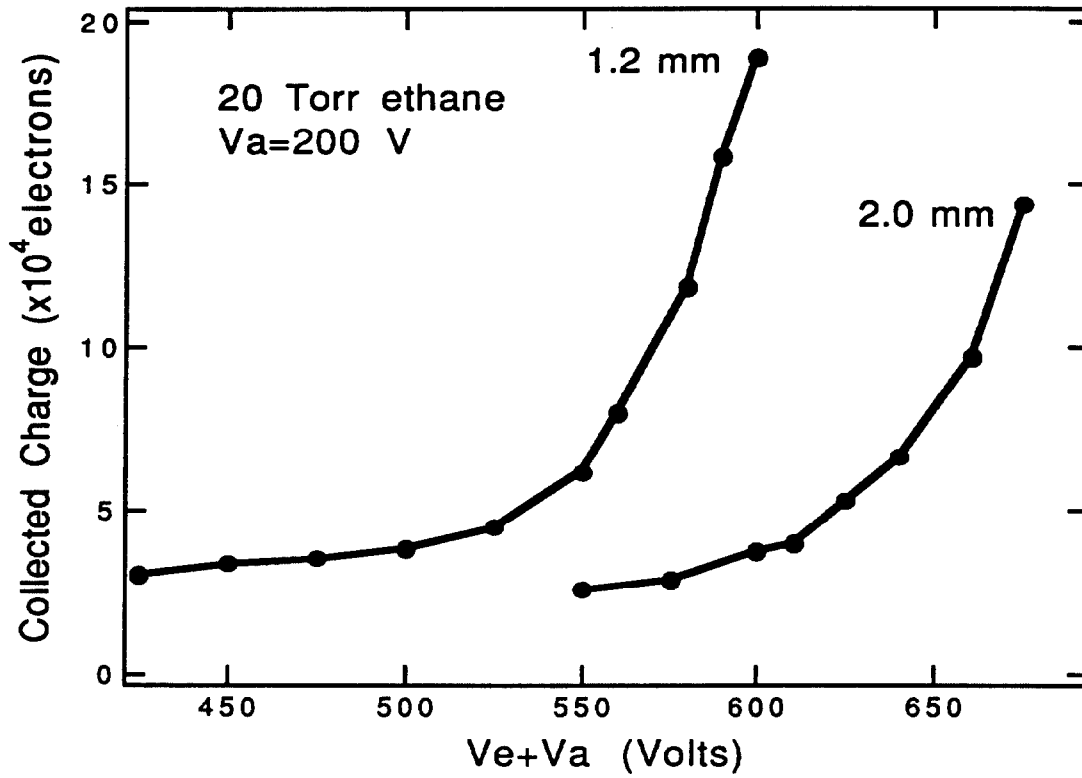


Figure 9

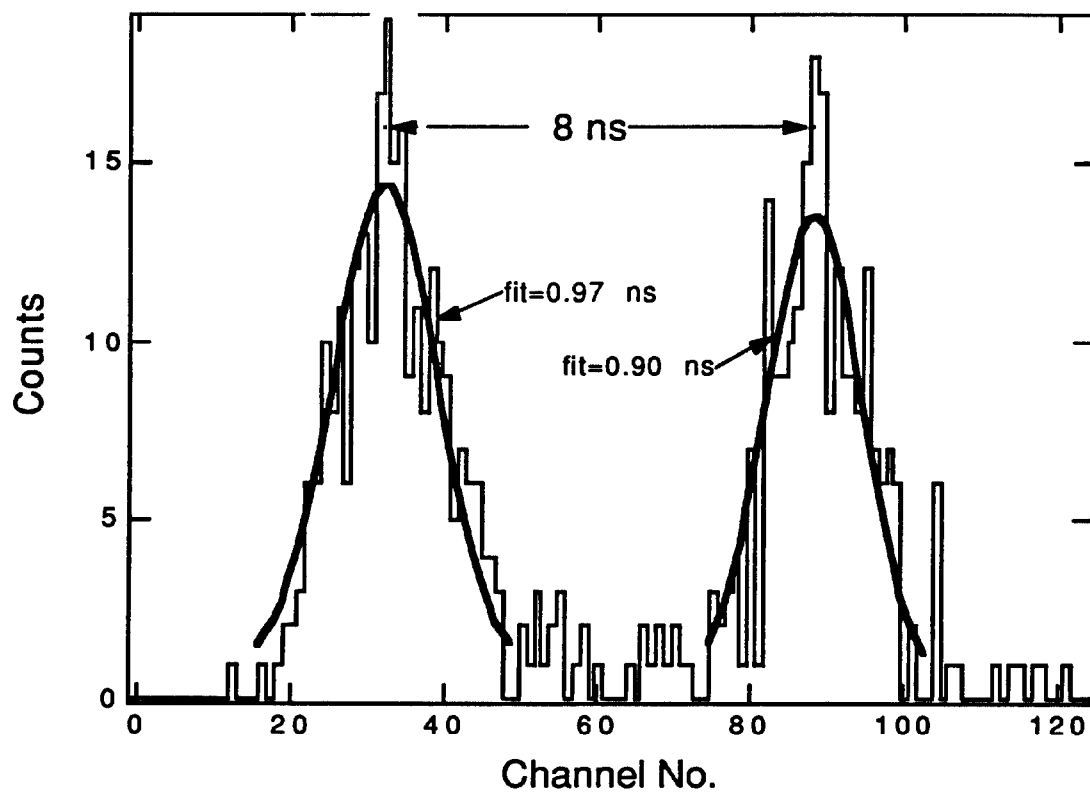


Figure 10